Research Article

Journal of Environmental Nanotechnology

Comparison of Organic and In-organic Phase Change Materials on Curing Time and Mechanical Properties of Geopolymer Bricks in Passive Solar Dryers

Jeevan Ashok kumar[1], Sattanathan Muthuvel[2], Ranjitharamasamy Sudhakarapandian[3], Gopinath Govindan Radhakrishnan[4] and Muthiah Muthukannan[5*]

[1]Department of Mechanical Engineering, Anna University, Madurai, TN, India
[2]Department of Mechanical Engineering, Kalasalingam Academy of Research and Education, Srivilliputhur, TN, India
[3]Department of Mechanical Engineering, Vellore Institute of Technology, Vellore, TN, India
[4]Department of Mechanical Engineering, M. Kumarasamy College of Engineering, Karur, TN, India
[5]Department of Civil Engineering, KCG College of Technology, Chennai, TN, India
Received: 10.12.2024 Accepted: 26.03.2025 Published: 30.03.2025
*muthukannan_research@rediffmail.com

ABSTRACT

Conventionally, phase change materials (PCM) are used as energy storage materials for latent and sensible heat in solar applications. PCM are generally classified as organic and inorganic. In this work, an organic PCM like paraffin wax and an inorganic PCM like manganese chloride tetrahydrate have been compared in terms of curing time and mechanical properties of Geopolymer bricks (GPB) obtained from fly ash, ground granulated blast furnace slag, Rice husk ash, and Nano silica, which are a target in construction industries for their reliable properties, when compared to conventional cement and sand bricks. The novelty of this work is to use an inorganic PCM in a Solar dryer to cure GPB, find its effect on the mechanical properties of GPB, and finally compare it with Organic PCM. It has been experimentally observed that GPB in Solar dryers with Inorganic PCM shows higher curing time, lesser compressive strength, lesser tensile strength, and lesser flexural strength when compared to GPB in Solar dryers with Organic PCM. The present study was also performed using ANSYS simulation software to correlate with experimental values. Simulation results predict a significant variation from experimental values, demanding more accuracy in simulation modeling. In conclusion, organic PCM performs better than inorganic PCM based on curing time, properties, and cost of the GPB in applications like construction, structural, and buildings.

Keywords: Geopolymer Bricks (GPB); Phase Change Materials (PCM); Manganese chloride tetra hydrate; Fly ash; Ground Granulated Blast Furnace Slag (GGBS); Rice husk ash.

1. INTRODUCTION

Solar energy is an excellent alternate energy source compared to other forms of energy, especially in areas like drying and heating. Generally, Solar energy is far better than conventional methods like electrical and open sun drying methods (Partheeban *et al.* 2024). In construction sectors, solar energy can reduce curing time, which is the time taken to remove moisture content and gain sufficient strength. Due to its abundance, solar energy is a target in construction sectors to cure bricks on a large-scale basis (Emrani and Berrada, 2024). Solar energy can be employed in construction sectors for hydrothermal curing bricks from waste management (Mostafa *et al.* 2024). The use of Solar energy sometimes imposes risks based on extremely hot climatic conditions (Juhola *et al.* 2024). Also, solar energy used for drying bricks has time limits in construction sectors, which can be overcome by using proper PCM, which is characterized by its latent heat, leading to thermal energy storage Mariela (Vega *et al.* 2024). Organic and Inorganic types of PCM are generally employed wherever thermal energy storage is needed (Ismail *et al.* 2024). Organic PCM and In-organic PCM find their applications in areas like building sectors (Bharathiraja *et al.* 2024). Paraffin wax is applied in load regulations as a building envelope Qudama (Al-Yasiri *et al.* 2021). PCM, like Manganese chloride tetrahydrate, finds its applications in sectors like the construction of residential buildings (Min *et al.* 2022). Emissions from conventional sand and cement brick industries also play a vital role in climatic changes in our ecosystem, leading to extremely hot and dry conditions (Fort and Cerny, 2020). GPB, introduced by Davidovits, was obtained by activating high-alumina silica-rich materials in an alkaline solution (consisting of sodium or potassium silicate and sodium or potassium hydroxide) (Bharath *et al.* 2023). It is similar to ceramic composites, with a link between alumina and silica. Geopolymer-based concrete based on fly ash has the potential to replace ordinary Portland cement (OPC) based concrete with comparable structural qualities in the construction industry. Nuclear power plant waste from power generation sectors can generate GPB, which are far free from emissions and exhibit excellent properties compared to conventional bricks (Kaliappan *et al.* 2024). Construction industries need GPBs that utilize less energy and produce less pollution, which inculcates hybrid Solar dryers in construction applications for curing bricks Nour Bassim (Frahat *et al.* 2024). Rice husk ash, Nano clay, and granite dust are potent substitutes for cement mortars to reduce emissions (Chen *et al*. 2024). Nano silica, a robust material in construction applications, finds its way to contributing to the development of GPB (Siba and Shyamal, 2024). Applications of GPB as a substitute for cement and sand bricks come under the scanner of modified guidelines of GPB concrete mix design using Indian standards Resha Kasim (Vellattu *et al.* 2024). The use of clean and green energy, like Solar energy, aided by energy storage materials in the curing process of GPB, forms a research platform to substitute conventional bricks in terms of performance, sustainability, and cost management in construction sectors. Also, Nano PCM has found its applications in energy storage under fluctuating loadings in Solar PV panels (Tripathi *et al.* 2024). Polymer matrix composites and ceramic hybrid polymer matrix composites have wide applications in the areas of thermal energy storage (Ramesh *et al.* 2023; Seeniappan *et al.* 2023). Polymer-based composite materials have always been attractive due to their potent properties compared to metals and alloys in thermal applications (Selvakanmani *et al.* 2024). This work deals with curing time and mechanical properties of GPB under a Solar dyer with PCM like Manganese Chloride Tetra Hydrate and compares GPB under a Solar dyer with Paraffin wax as PCM (Singh *et al*. 2024; Jeevanantham *et al*. 2024). Both the PCMs have been selected for comparison because their melting points are very close, which is evident from Table 1.

Fig. 1: Solar dryer

2. MATERIALS AND METHODOLOGY

A fabricated Solar dryer for the purpose of experimentation is shown in Fig.1. The dryer setup consists of an iron stand, UV-coated parabolic polycarbonate sheets, an aluminum frame, and a Cudappah stone to maintain a uniform curing atmosphere inside the dryer. A solar-powered photovoltaic (PV) panel fan automatically turns on and off during the curing process to control the degree of temperature saturation. Table 1 shows the properties of paraffin wax and manganese chloride tetrahydrate.

Table 1. Properties of paraffin wax

PCM	Melting Temperature (°C)	Density (kg/m^3)	Specific Heat (J/kgK)	Thermal Conductivity (W/mK)	Latent Heat of Fusion (kJ/kg)
Paraffin wax	57.5	915	2005	0.225	205
Manganese chloride tetra-hydrate	58	210	2290	0.113	176

The method of preparation, raw material proposition and chemical proposition of ingredients of GPBs are shown in Fig. 2, Table 2, and Table 3.

Fig. 2: Chemcial ingredients of GPB (a) Sodium carbonate (b) Fly ash (c) GGBS (d) Nano silica (e) Sodium hydroxide (f) Coarse aggregate and (g) Rice husk ash (h) M sand

Table 2. Raw material proportion of GPB (Percentage by volume)

Material	Weight in kg/m^3	GPB1	GPB2
Fly ash	285	70%	52%
GGBS	165	30%	30%
Rice husk ash	82.4	-	15%
Nano silica	16.4	-	3%

Table 3. Chemical proportion of GPB (Percentage by weight)

	SiO_2	Al_2O_3	CaO	MgO	K_2O	Fe_2O_3	TiO_2	Na_2O	SO_3
Fly Ash	52	27	3.5	9.25	7.5	1.55	0.845	0.725	0.545
GGBS	35	14	36	7.5	0.545	0.45	0.725	0.25	1.65
Nano silica	90.5	0.082	0.059	0.081	0.011	0.02	-	0.89	0.23
Rice husk ash	85.85	0.19	1.95	0.375	1.98	0.09	-	0.39	-

The particle sizes for fly ash, ground granulated blast furnace slag, Nano silica, and rice husk ash were 44 µm, 12 µm, 72 nm, and 48 µm, respectively. The ignition loss for fly ash and ground granulated blast furnace slag, Nano silica, and rice husk ash was 0.7%, 0.69%, 1.1%, and 1.5%, respectively. The alkaline activator for the polymerization process consists of distilled water, sodium hydroxide (96 % purity and 12 morality), and sodium silicate. The chemical proposition of fly ash, ground granulated blast furnace slag, Nano silica, and rice husk ashes are tabulated in Table 3. Sodium hydroxide (NaOH) added to distilled water was kept in the bowl for 24 hours. After 24 hours, the sodium silicate (Na_2SiO_3) solution was mixed and stirred well. After 60 minutes, this solution was mixed with fly ash, ground granulated blast furnace slag, Nano silica, rice husk, coarse aggregate, and fine aggregate sand in appropriate quantities. Manufactured sand forms the medium for the final concrete or mortar mix, in which the primary activator, sodium metal, exhibits binding action in the polymerization process. Silicon dioxide and aluminum oxide play a crucial role in shaping the microstructure of GPB. Fig. 3 shows how the mixture looks after all ingredients are well stirred.

Fig. 3: (a) Stirred mixture (b) Final mixture in mould

The above-mentioned method is for preparing GPB2, and when Nano silica and rice husk ash are removed from precursors, it forms the method for preparing GPB1. Fig. 4 depicts the cubic, cylindrical, and rectangular prism specimens prepared for experimentation. Fig. 5 depicts the specimen, which is kept in a Solar dryer over Cuddapah stone along with manganese chloride tetrahydrate.

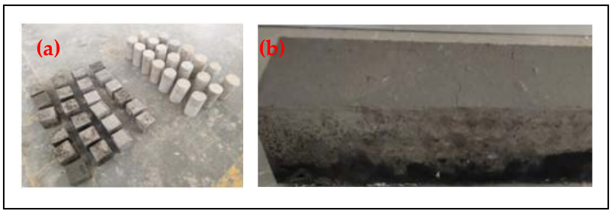

Fig. 4: (a) Cubic and cylindrical specimen (b) Rectangular prismatic specimen

Fig. 5: GPB with manganese chloride tetra hydrate kept in solar dryer

Solar energy incident on the dryer gets converted into convection, an active form of heat energy transfer, and radiation, a passive form of heat energy transfer, during the curing process of GPB. PCM's sensible and latent heat handles the entire curing process of GPB. At the beginning of the curing process, the GPB exhibits variations in weight, as measured by the balancing machine, and later gets stabilized. Further, the GPB was allowed to develop proper strength at room temperature for 28 days and taken for testing. The dimensions of the specimens as per ASTM standards used for testing are shown in Table 4.

Table 4. Specimen standards (Dimensions in cm)

Test	Geometry	Length	Breadth	Height	Diameter	Standard
Tensile split strength	Cubic	10	10	10		ASTM C496-96
Compressive strength	Cylindrical	20			10	ASTM E9-19
Flexural strength	Rectangular prismatic	50	10	10		ASTM D790-17

The number of specimens for each test is two for the sake of accuracy of readings. Fig. 6 show the setup used for testing compression (Fig. 6a), tension (Fig. 6b), and flexural (Fig. 6c).

Fig. 6: (a) GPB in tension split test (b) GPB in compression test (c) GPB in flexural test

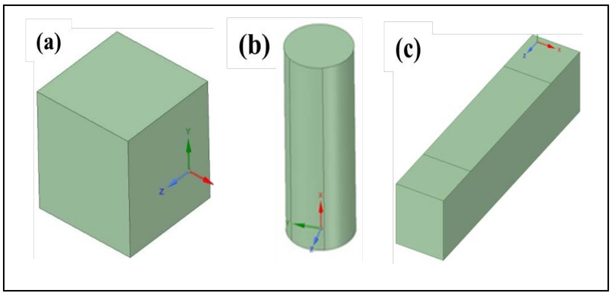

Fig. 7: (a) Geometry of Cubic specimen, (b) Cylindrical specimen and (c) Rectangular prism specimen

2.1 Simulation

For GPB, the research works available in the literature are entirely related to experimental techniques. Very few works have been reported under the simulation of mechanical testing of GPB. Since the geometry of GPB is simple and regular, like cubic, cylindrical, and rectangular prismatic for testing, a simple investigational work has been performed on mechanical testing of GPB by simulation using ANSYS-WORKBENCH. Figs. 7, 8, 9, and 10 show geometry, mesh, boundary conditions, and loading, respectively.

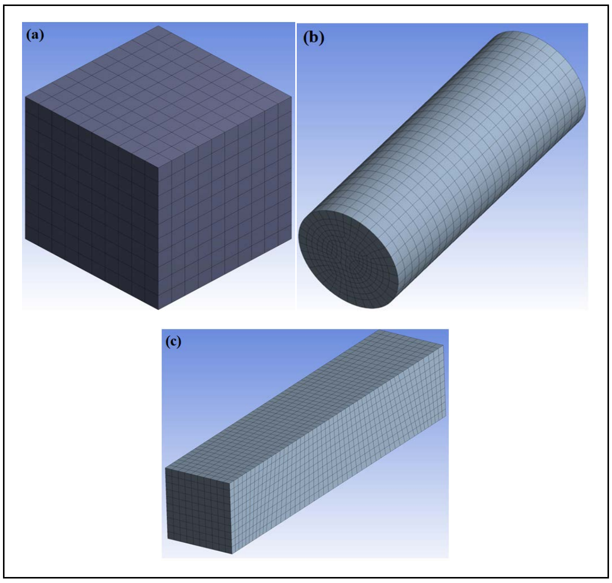

Fig. 8: (a) Mesh of Cubic specimen (b) Cylindrical specimen (c) Rectangular prism specimen

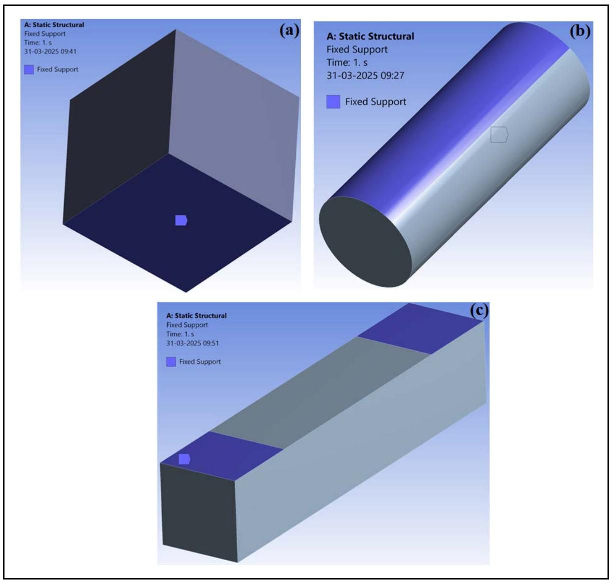

Fig. 9: (a) Fixed supports on Cubic specimen, (b) Cylindrical specimen, (c) Rectangular prism specimen

For cubic, cylindrical, and rectangular prismatic specimens, the meshing has been done by program control method to generate 1000 elements with 4961 nodes, 6210 elements with 26830 nodes, and 5000 elements with 23441 nodes, respectively. Regarding material properties, the GPB has been modeled by a percentage mixture of volume fraction to calculate the effective modulus of elasticity and Poisson's ratio (Jeevanantham *et al.* 2024). The effective properties used for simulation are shown below in Table 5.

$$E = 0.7*E_{flyash}+0.3*E_{GGBS}$$

$$\mu = 0.7*\mu_{flyash}+0.3*\mu_{GGBS}$$

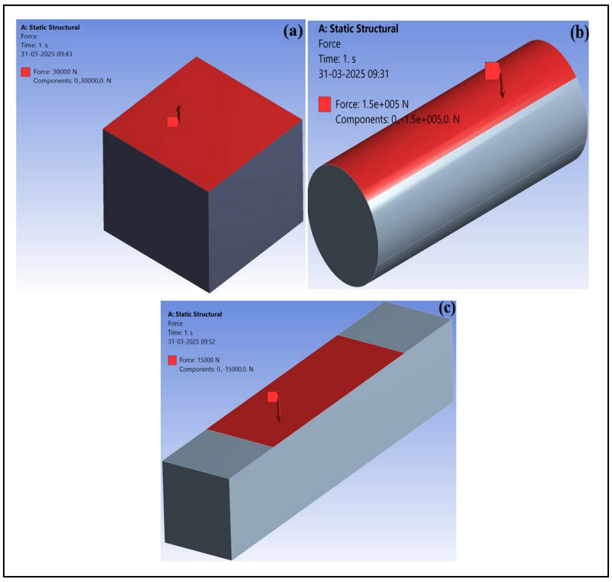

Fig. 10: (a) Loads applied on cubic specimen, (b) Cylindrical specimen and (c) Rectangular prism specimen

Table 5. Effective material properties of GPB1 And GPB2

GPB	Modulus of Elasticity (MPa)	Poisson's Ratio	Effective Modulus of Elasticity (MPa)	Effective Poisson's Ratio
Fly ash	25000	0.22	32500	0.2350
GGBS	50000	0.27		

3. RESULTS AND DISCUSSION

The results of mean value of two specimens in each test have been established in Fig. 11, 12, 13 and 14 with the following inference.

As per the observations from Fig. 11, it is understood that GPB under Solar dryer with Manganese Chloride Tetra Hydrate as PCM consumes almost 22.5 hours for both GPB1 and GPB2 (Ramachandran *et al.* 2012; Jeevan *et al*. 2023; Deb *et al*. 2015). As per Indian standards for GPB concrete mix design, the target compressive strength for conventional GPB is around 30 MPa (Ramachandran *et al.* 2012; Jeevan *et al.* 2023), but the experimental result obtained was 40.5 MPa and 43.5 MPa for GPB1 and GPB2 in Solar dryer with Manganese Chloride tetrahydrate as PCM, respectively as shown in Fig. 12. Further, tensile split strength of 2.8 MPa and 3.9 MPa and flexural strength of 5.5 MPa and 6 MPa were obtained for GPB1 and GPB2, respectively as shown in Fig. 13, 14.

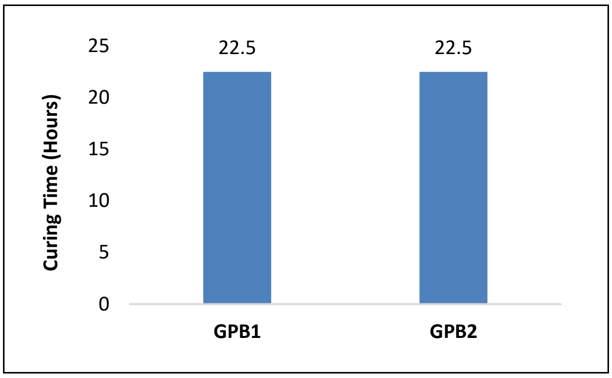

Fig. 11: Curing time for GPB1 and GPB2

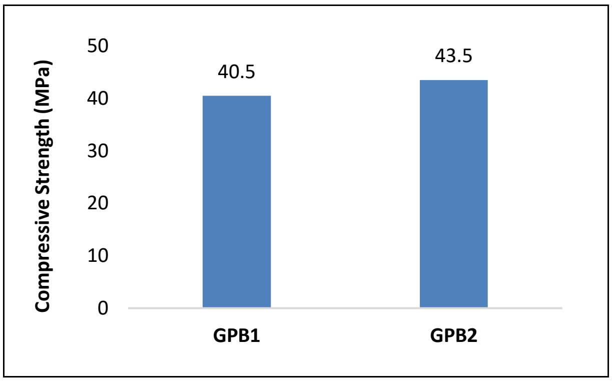

Fig. 12: Compressive strength comparison for GPB1 and GPB2

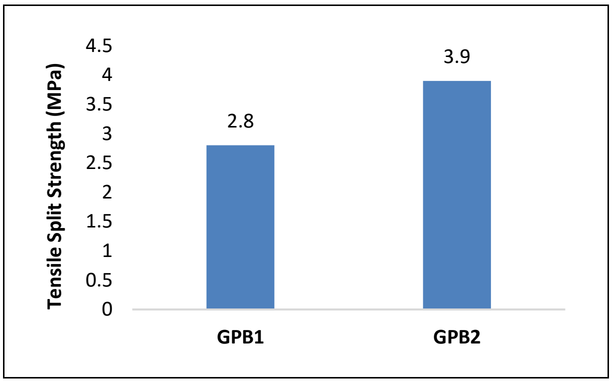

Fig. 13: Tensile split strength comparison for GPB1 and GPB2

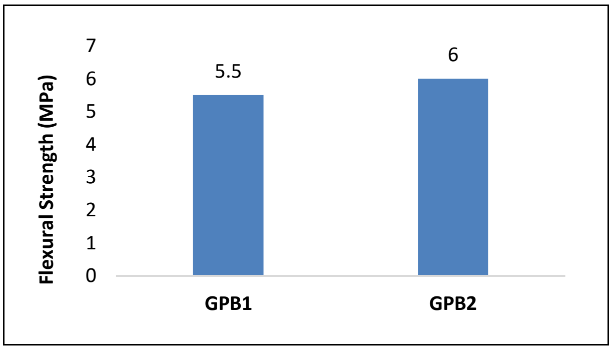

Fig. 14: Flexural strength comparison for GPB1 and GPB2

Experimentally, it is evident from Fig. 11, 12, 13, and 14 that GPB1 in Solar dryer with In-organic PCM shows higher curing time by 30 minutes, lesser compressive strength by 2.41 %, lesser tensile strength by 16.42 % and lesser flexural strength by 11.29 %, when compared to GPB1 in Solar dryer with Organic PCM (Albitar *et al.* 2015; Tripathi *et al.* 2024; Ramesh *et al.* 2023; Capossio *et al.* 2022; Ramachandran *et al.* 2012; Jeevan *et al.* 2023; Deb *et al.* 2015). Similarly, GPB2 in a Solar dryer with In-organic PCM shows higher curing time by 30 minutes, lesser compressive strength by 3.33 %, lesser tensile strength by 13.33 %, and lesser flexural strength by 7.69 %, when compared to GPB2 in Solar dryer with Organic PCM (Albitar *et al.* 2015; Tripathi *et al.* 2024; Ramesh et al. 2023; Capossio et al. 2022; Ramachandran *et al*. 2012; Jeevan *et a*l. 2023; Deb *et al.* 2015). For Solar dryer with Organic PCM, GPB2 shows 8.43% higher compressive strength, 34.32% higher tensile split strength and 4.84% higher flexural strength, when compared to GPB1. Similarly, for Solar dryers with Inorganic PCM, GPB2 shows 7.41% higher compressive strength, 39.28% higher tensile split strength, and 9.09% higher flexural strength than GPB1.

The case taken for the study in the simulation was GPB1 under a Solar dryer with Inorganic PCM. Directional displacement plots for X, Y, and Z directions for compression, tensile, and flexural loading, respectively, are shown in Figs. 15, 16, and 17.

The maximum and minimum values of directional displacement (X, Y and Z) plots for all the three types of loading are shown below in Table. 6.

Table 6. Directional displacement (X, Y and Z) plots

GPB1	Solar dryer (Manganese chloride tetrahydrate)					
	Compression Loading (150 kN)		Tensile Split Loading (30 kN)		Flexural Loading (15 kN)	
	Min	Max	Min	Max	Min	Max
X	-0.0036	0.0036	-0.0011	0.0011	-0.0006	0.0006
Y	-0.0163	0	0	0.0091	-0.0114	$7.7283e^{-5}$
Z	-0.0085	0.0011	-0.0011	0.0011	-0.0032	0.0029

In the stress plots shown in Fig. 18, at specific constraint locations like fixed supports, the equivalent stress values are unrealistic due to stress concentrations. So, the values slightly lesser than the peak values from the simulation have been considered for comparison with experimentation values. So, from Fig. 20, equivalent stress shows a value of 31.554 MPa against the experimental value of 40.5 MPa in the compression test with 22.1% variation, 3.654 MPa against the experimental value of 2.8 MPa in the tensile test with 30.5% variation and 5.6595 MPa against the experimental value of 5.50 MPa in flexural testing with 2.9% variation, respectively.

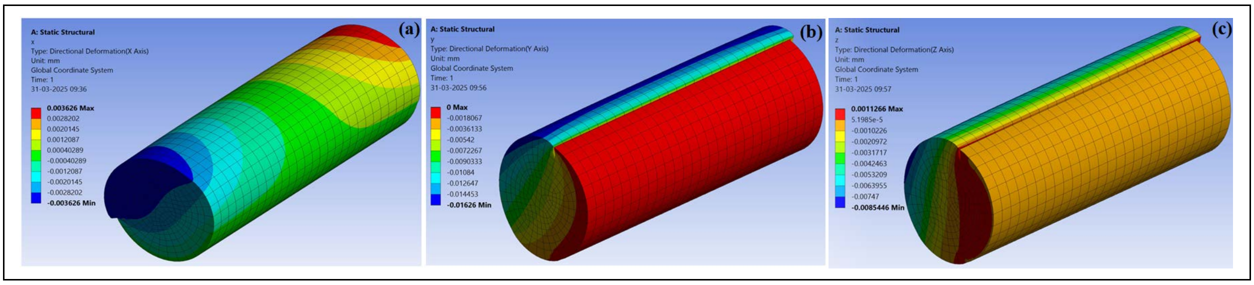

Fig. 15: Displacement plots for cylindrical specimen compression loading (a) X-direction (b) Y-direction (c) Z-direction

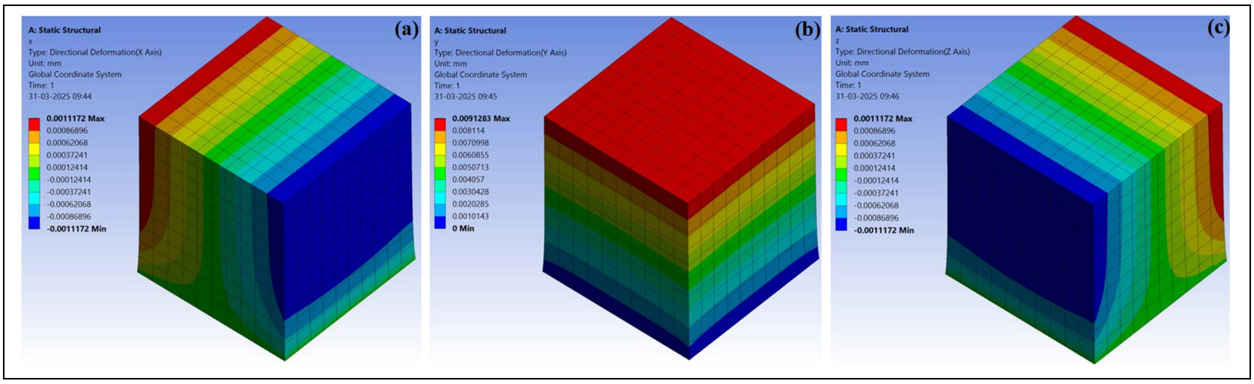

Fig. 16: Displacement plots for cubic specimen tensile loading (a) X-direction (b) Y-direction (c) Z-direction

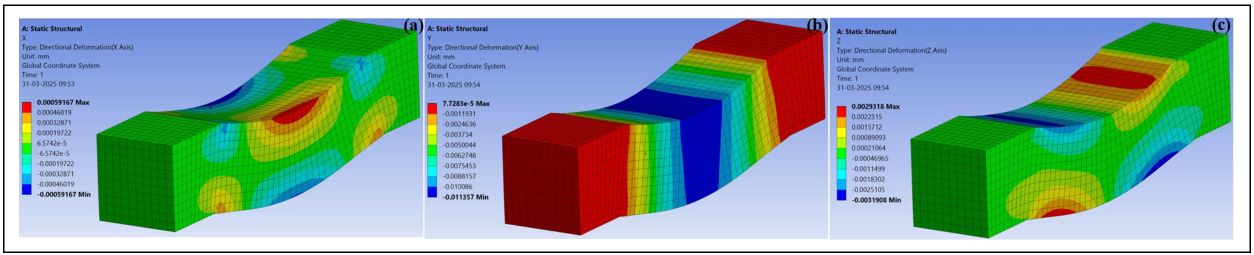

Fig.17: Displacement plots for rectangular prism specimen flexural loading (a) X-direction (b) Y-direction (c) Z-direction

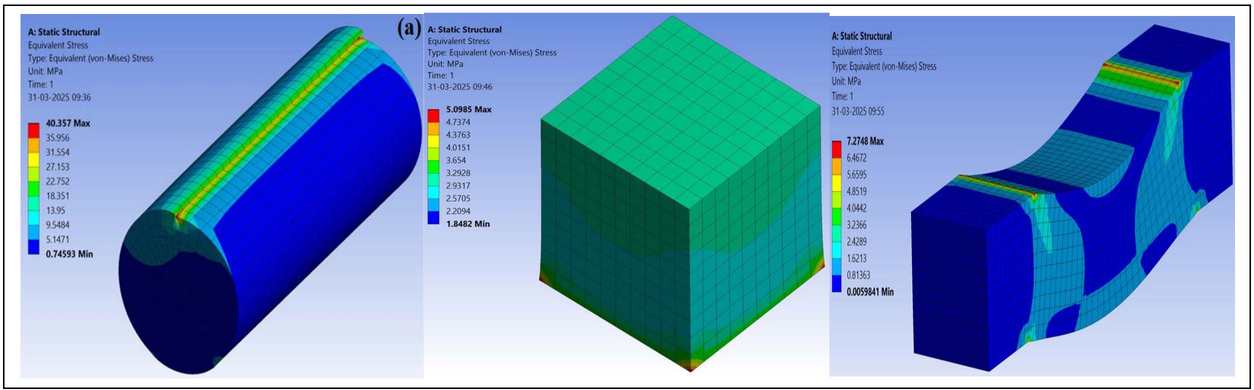

Fig. 18: Equivalent stress plots for (a) cylindrical specimen compression loading (b) cubic specimen tensile loading (c) rectangular prism specimen flexural loading loading

It is evident from Tables 7, 8, 9, and 10, respectively, that GPB under a Solar dryer with Manganese Chloride Tetra Hydrate as PCM shows more curing time and lower mechanical properties like compressive strength, tensile split strength, flexural strength, respectively, when compared to GPB under a Solar dryer with Paraffin wax as PCM (Ramachandran *et al.* 2012; Jeevan *et al.* 2023; Deb *et al.* 2015).

Table 7. Curing time comparison for GPB1 and GPB2

GPB	Solar dryer (Paraffin Wax)	Solar dryer (Manganese chloride tetrahydrate)
	Curing Time (Hours)	Curing Time (Hours)
GPB1	22	22.5
GPB2	22	22.5

Table 8. Compressive strength comparison for GPB1 and GPB2

GPB	Solar dryer (Paraffin Wax)	Solar dryer (Manganese Chloride Tetra Hydrate)	Percentage difference w.r.t Paraffin wax
	Compressive Strength (MPa)	Compressive Strength (MPa)	
GPB1	41.5	40.5	2.41
GPB2	45.0	43.5	3.33

Table 9. Tensile split strength comparison for GPB1 and GPB2

GPB	Solar dryer (Paraffin Wax)	Solar dryer (Manganese Chloride Tetra Hydrate)	Percentage difference w.r.t Paraffin wax
	Tensile Strength (MPa)	Tensile Strength (MPa)	
GPB1	3.35	2.8	16.42
GPB2	4.50	3.9	13.33

Table 10. Flexural strength comparison for GPB1 and GPB2

GPB	Solar dryer (Paraffin wax)	Solar dryer (Manganese chloride tetrahydrate)	Percentage difference w.r.t Paraffin wax
	Flexural Strength (MPa)	Flexural Strength (MPa)	
GPB1	6.20	5.5	11.29
GPB2	6.5	6	7.69

The lower latent heat of fusion leads to lesser heat storage and a relatively more extraordinary ambiance inside the solar dryer, leading to a delayed curing process. Also, due to lesser heat storage, the particles inside GPB get weakly bonded, exhibiting lesser mechanical properties (Deb *et al.* 2015). Comparing values of curing time between GPB1 and GPB2 for both the PCM cases, no difference is noted, while properties values illustrate differences. GPB2 shows higher properties in both the PCM cases than GPB1. This is due to the addition of rice husk ash and Nano silica, which gives better bonding and interlocking effects between the particles of GPB, respectively (Yılmazer *et al.* 2023). Adding further Nano silica to GPB by more than 3% by volume is not recommended because it may lead to reduced properties due to its brittle nature (Yılmazer *et al.* 2023). This PCM-based Solar dryer curing is introduced to overcome the degradation effects of GPB while curing in open sun drying (extremely high temperatures) and unexpected changes in climatic conditions.

As the simulation is an investigational study, we have not modeled the fracture criterion. So, the energy required for fracture is not captured in this study. Instead, we have performed an analysis to capture the behavior and distribution of field variables like displacement (X, Y, and Z) and equivalent stress. In equivalent stress plots, values show significant deviation from compression tension test data and less deviation from flexural test data (Jeevanantham *et al.* 2024), as shown in Table 11.

Table 11. Comparison between simulation and experiment

GPB	Solar dryer (Manganese chloride tetrahydrate)					
	Compression Strength (MPa)		Tensile Split Strength (MPa)		Flexural Strength (MPa)	
	ANSYS	Exp.	ANSYS	Exp.	ANSYS	Exp.
GPB1	31.554	40.5	3.654	2.8	5.6595	5.50
% Diff	22.1%		30.5%		2.9%	

4. CONCLUSION

For GPB, a Solar dryer with Manganese Chloride Tetrahydrate as PCM consumes 22.5 hours of curing time, and a Solar dryer with Paraffin Wax consumes 22 hours of curing time.

As per Indian standards for Geopolymer concrete mix design, the target compressive strength is around 30 MPa, but for GPB dried in Solar dryer with Manganese Chloride Tetra Hydrate as PCM, the experimental result obtained was 40.5 MPa for GPB1 and 43.5 MPa for GPB2, respectively.

The above two conclusions suggest that GPB is favorable for construction, buildings, and structural steel and is an excellent alternative to conventional sand and cement bricks. GPB, under Solar drying with Manganese Chloride Tetra Hydrate as PCM, shows higher curing time, lesser compressive strength, tensile split strength and flexural strength than Solar drying with Paraffin Wax as PCM. So, Organic PCM (Paraffin wax) performs better than Inorganic PCM (Manganese Chloride Tetra Hydrate). While comparing proprties of GPB1 and GPB2, GPB2 shows better properties due to addition of rice husk and nano-silica (upto 3%) which enhances mechanical properties. Adding nano-silica greater than 3% is not recommended because in extreme hot conditions it may lead to degradation of properties. The simulation study results will closely match the experiment results only if the fracture criterion is modeled into them, which forms the scope of future work.

FUNDING

There is no funding source.

CONFLICT OF INTEREST

The authors declared no conflict of interest in this manuscript regarding publication.

REFERENCES

Albitar, M., Visintin, P., Mohamed, A. M. S. and Drechsler, M., Assessing behaviour of fresh and hardened geopolymer concrete mixed with class-F fly ash, *KSCE J. Civ. Eng.*, 19(5), 1445–1455(2015). https://doi.org/10.1007/s12205-014-1254-z

Al-Yasiri, Q. and Szabo, M., Paraffin As a Phase Change Material to Improve Building Performance: An Overview of Applications and Thermal Conductivity Enhancement Techniques, *Renew. Energy Environ. Sustain.*, 6, 1-13(2021). https://doi.org/10.1051/rees/2021040

Bharath, R. G., Naveen, K. G., Manjeet Kharub, Cryogenic processing of AISI P20 tool steel: Evaluation of mechanical properties and microstructure, *Mater. Today Proc.,* (2023). https://doi.org/10.1016/j.matpr.2023.02.274

Bharathiraja, R., Ramkumar, T., Selvakumar, M. and Radhika, N., Thermal characteristics enhancement of Paraffin Wax Phase Change Material (PCM) for thermal storage applications, *Renewable Energy*, 222, 119986(2024). https://doi.org/10.1016/j.renene.2024.119986

Capossio, J. P., Fabani, M. P., Reyes-Urrutia, A., Torres-Sciancalepore, R., Deng, Y., Baeyens, J., Rodriguez, R. and Mazza, G., Sustainable Solar Drying of Brewer's Spent Grains: A Comparison with Conventional Electric Convective Drying, *Proc.*, 10(2), 339(2022). https://doi.org/10.3390/pr10020339

Chen, K., Liu, Q., Chen, B., Zhang, S., Ferrara, L. and Li, W., Effect of raw materials on the performance of 3D printing geopolymer: A review, *J. Build. Eng.*, 84, 108501(2024). https://doi.org/10.1016/j.jobe.2024.108501

Deb, P. S., Prabir, K. S. and Salim, B., Effects of nano-silica on the strength development of geopolymer cured at room temperature, *Constr. Build. Mater.*, 101(1), 675–683(2015). https://doi.org/10.1016/j.conbuildmat.2015.10.044

Emrani, A. and Berrada, A., A comprehensive review on techno-economic assessment of hybrid energy storage systems integrated with renewable energy, *J. Energy Storage*, 84(8), 111010(2024). https://doi.org/10.1016/j.est.2024.111010

Fort, J. and Cerny, R., Transition to circular economy in the construction industry: Environmental aspects of waste brick recycling scenarios, *Waste Manage.*, 118, 510–520(2020). https://doi.org/10.1016/j.wasman.2020.09.004

Frahat, N. B., Awed, A. S., Kassem, S. M., Abdel, M. M. I. A. and Mohamed, O. I. O., Innovative shielding solutions by geopolymer paste and fly ash as effective substitution of cement materials for sustainable protection, *J. Build. Eng.*, 87, 108977(2024). https://doi.org/10.1016/j.jobe.2024.108977

Ismail, A., Bahmani, M., Chen, X. and Wang, J., An organic-inorganic hybrid microcapsule of phase change materials for thermal energy storage in cementitious composites, *Constr. Build. Mater.*, 416, 135289(2024). https://doi.org/10.1016/j.conbuildmat.2024.135289

Jeevan, A. K., Sattanathan, M., Issac, S. R. V., Ramoni, M., Shanmugam, R. and Ranjitharamasamy, S. P., Mechanical Properties Comparison of Geo Polymer Brick Dried by Electrical and Passive Solar Devices With Phase Change Material (Paraffin Wax), *Processes*, 12(1), 28(2023). https://doi.org/10.3390/pr12010028

Jeevanantham, S., Seeniappan, K. L. Natrayan, and M., Muthukannan, Influence of peanut husk derived heat-treated Si3N4 on load bearing properties of basalt fibre-reinforced polyester composite, *J. Aust. Ceram. Soc.,* 1-13(2024). https://doi.org/10.1007/s41779-024-01104-9

Juhola, S., Laurila, A., Groundstroem, F. and Klein, J., Climate risks to the renewable energy sector: Assessment and adaptation within energy companies, *Bus. Strat. Env.*, 33(3), 1906–1919(2024). https://doi.org/10.1002/bse.3580

Kaliappan, S., Paranthaman, V., Kamal, M. D. R., Avv, S. and Muthukannan, M., A Novel Approach of Particle Swarm and ANT Colony Optimization for Task Scheduling in Cloud, In: 2024 14th International Conference on Cloud Computing, Data Science and Engineering (Confluence), Noida, India, *2024 14th International Conference on Cloud Computing, Data Science & Engineering (Confluence),* 272–278 (2024a)., https://doi.org/10.1109/Confluence60223.2024.10463398

Min, K. E., Jang, J. W., Kim, J. K., Wern, C. and Yi, S., Thermophysical Properties of Inorganic Phase-Change Materials Based on MnCl2·4H2O, *Appl. Sci.*, 12(13), 6338(2022). https://doi.org/10.3390/app12136338

Mostafa, S. A., El-Gamal, S. M. A., Mohsen, A., Ramadan, M., Wetwet, M. M., Deghiedy, N. M., Swilem, A. E., and Hazem, M. M., Towards a green climate: Production of slag–red brick waste-based geopolymer mingled with WO_3 nanoparticles with bio-mechanical achievements. *Constr. Buil. Mater.*, 13, 134909(2024). https://doi.org/10.1016/j.conbuildmat.2024.134909

Partheeban, P., Jegadeesan, V., Manimuthu, S. and Chella G. C., Cleaner production of geopolymer bricks using Solar-LPG hybrid dryer, *J. Cleaner Prod.*, 442, 141048(2024). https://doi.org/10.1016/j.jclepro.2024.141048

Ramachandran, A., Venkatasubramani, R., Venkataraman, S. and Rangan, B. V., Modified guidelines for geopolymer concrete mix design using Indian standard, *Artic. Asian J. Civ. Eng,*, 13, 353–364(2012). https://doi.org/10.1007/978-81-322-2187-6_123

Ramesh, V., Karthik, K., Arunkumar, K., Unnam, N.K., Ganesh, R. and Rajkumar, C., Effect of sawdust filler with Kevlar/basalt fiber on the mechanical properties epoxy–based polymer composite materials, *Mater. Today Proc.,* 72, 2225-2230(2023). https://doi.org/10.1016/j.matpr.2022.09.208

Selvakanmani, S., Seeniappan, K. and Muthukannan, M., Recognition of Cyber Physical Systems Through Network Security for Wireless Sensor Networks: Using Artificial InItelligence in Cyber Physical Systems. In Intelligent Solutions for Sustainable Power Grids, *Global Sci. Publ. Int. Acad.*, 272-286(2024). https://doi.org/10.4018/979-8-3693-3735-6

Siba, S. C. and Shyamal, G., A comprehensive review on the factors influencing engineering characteristics of lightweight geopolymer concrete, *J. Build. Eng.*, 86, 108887(2024). https://doi.org/10.1016/j.jobe.2024.108887

Singh, P., Vikas, M., Natrayan, L., Kandukuri, S. Seeniappan, K., Muthiah, M. and Gopinath, R., Prediction of groundwater contamination in an open landfill area using a novel hybrid clustering-based AI *model Environ. Prot. Eng.*, 50(1), (2024). https://doi.org/10.37190/epe240106

Tripathi, A. K., Aruna, M., Elumalai, P. V., Karthik, K., Khan, S. A., Asif, M. and Rao, K. S., Advancing Solar PV panel power prediction: A comparative machine learning approach in fluctuating environmental conditions, *Case Stud. Therm. Eng.*, 59, 104459(2024). https://doi.org/10.1016/j.csite.2024.104459

Vega, M., Marín, P. E., Ushak, S. and Shire, S., Research trends and gaps in experimental applications of phase change materials integrated in buildings, *J. Energy Storage*, 75, 109746(2024). https://doi.org/10.1016/j.est.2023.109746

Vellattu, C. R. K., Ozhukka, P. F., Panakkal, T., Meethale, C. B., Kumari, P. and Valiya, P. S., Clean technology for sustainable development by geopolymer materials, *Phy. Sci. Rev., 9*(1), 327–342(2024). https://doi.org/10.1515/psr-2022-0194

Yilmazer, P. B., Numerical Analysis of Double Geopolymer Concrete Layer with Different Properties, *Int. J. Innovative Eng. Appl.,* 7(2), 195–200(2023). https://doi.org/10.46460/ijiea.1382611